

Article

L-Glutamine Coating on Antibacterial Cu Surface by Density Functional Theory

Maria Bouri and Christina Lekka *

Department of Materials Science and Engineering, University of Ioannina, 45110 Ioannina, Greece; maria.bouri1990@gmail.com

* Correspondence: chlekka@uoi.gr

Abstract: The protection of implant surfaces from biofilm and corrosion is crucial for osteogenesis and tissue engineering. To this end, an L-glutamine-based green corrosion inhibitor with recently established anticancer properties has been applied onto antibacterial Cu(111) surfaces that usually cover the Ti-based implants. Among several configurations, L-glutamine prefers the parallel to the surface orientation with the carbon chain along the [110] direction having the heteroatoms N and O atoms on top of Cu surface atoms, which is important for the creation of a planar two-dimensioned (2d) stable coating. L-glutamine forms well-localized, directional covalent-like bonded states (below -3 eV) with the Cu surface atoms, using mainly its backbone's N_1 atom that interestingly also shows electron charge occupation in the single-molecule highest occupied state, denoting its ability as an active center. The Mulliken analysis shows charge transfer from the molecule's N, C and Cu neighboring atoms towards the O atoms revealing the strong bond tendency of L-glutamine and therefore its ability to act as a corrosion inhibitor on the Cu surface. Additional L-glutamine adsorption results in intermolecular covalent bonding between the molecules, proving the ability of this amino acid to form a stable protective 2d organic coating on Cu(111). These results could be used for the design of a multifunctional hybrid (organic–metallic) coating with anticorrosion, anticancer and antibacterial properties suitable for many technological applications.

Keywords: L-glutamine; copper surface; DFT; corrosion; coating



Citation: Bouri, M.; Lekka, C. L-Glutamine Coating on Antibacterial Cu Surface by Density Functional Theory. *Crystals* **2023**, *13*, 1698. <https://doi.org/10.3390/cryst13121698>

Academic Editors: Zacharias G. Fthenakis and Nektarios N. Lathiotakis

Received: 4 December 2023
Revised: 13 December 2023
Accepted: 16 December 2023
Published: 18 December 2023



Copyright: © 2023 by the authors. Licensee MDPI, Basel, Switzerland. This article is an open access article distributed under the terms and conditions of the Creative Commons Attribution (CC BY) license (<https://creativecommons.org/licenses/by/4.0/>).

1. Introduction

The design of Ti-implant surfaces with biofilm and corrosion resistance is important for osteogenesis and tissue engineering [1–8]. Cu doping or coating has been successfully applied on Ti-based implant surfaces revealing antibacterial capability and enhancing bone repair and angiogenesis [1–4,7]. Despite biomaterials, the protection of a Cu surface from corrosion is critical for microelectronic devices, water supplies and environmental pollution although favored in architectural structures [8–11]. Organic compounds have been widely used as corrosion inhibitors on metallic surfaces providing low-cost opportunities to manufacturers and industry [8,10,12–16]. Researchers have shown that excellent organic inhibitors are those who cannot only donate electrons to the metallic surface's d orbital but are also able to accept free electrons, using their antibonding orbitals, in order to form feedback bonds [17]. These electronic interactions depend strongly on the electronic charge density distribution of the inhibitor and the metal surface. The organic molecule's highest charge density regions would preferably donate electrons to the partially filled or even vacant d orbital of the metallic surface resulting in donor–acceptor bonds [18], while these inhibitors' adsorption sites mainly occur due to the existence of active centers, such as (a) P, S, N and O atoms, (b) double or triple bonds and (c) aromatic rings [19].

Amino acids are important corrosion inhibitors because they are biodegradable, non-toxic, relatively cheap and abundant [12–15,17,18,20–27]. Several researchers have investigated the inhibitory potential of some amino acids revealing their efficiency as green

corrosion inhibitors [18,24,26,27]. L-glutamine is a conditionally essential amino acid present abundantly throughout the body and is involved in many metabolic processes. The L-glutamine's adsorption behavior on metallic surfaces has been studied in the past both experimentally and theoretically [14,17,25,27]. Research that focused on the corrosion protection of iron surfaces has shown that L-glutamine's backbone N and O atoms can interact with the surface's atoms not only through their lone pair electrons but also through their p electrons that are hybridized with the empty 3d orbital to form a protective layer [25]. Interestingly, the L-glutamine molecule uses either the aldehyde function to interact with the vacant Fe orbital [14,17] or both N and O atoms [25]. Nevertheless, a systematic theoretical study of L-glutamine on Cu surfaces is limited. It was experimentally suggested that the amino acids are physically adsorbed on the copper following Langmuir isotherm [22]. Scanning tunneling microscopy images reveal the adsorption of amino acids on copper surfaces like lysine and alanine to form parallel ordered superstructures like lysine stripes parallel to [110] on Cu(001), while similar behavior stands for glycine on Cu(111) [24]. Moreover, the role of glutamine metabolism as a therapeutic strategy for cancer has been proposed, since cancer cells depend on glutamine for survival and proliferation [28]. Therefore, a fundamental understanding of the adsorption and creation of a 2d L-glutamine organic coating on Cu is critical providing both anticorrosion and anticancer properties on the Ti-implant. Although there are experimental and theoretical data available for amino acids, including L-glutamine, basically on steel and iron surfaces, theoretical studies on full d-electron metallic surfaces like Cu, Au and Ag to our knowledge are limited. The adsorption of aromatic-based molecules on Cu, Au and Ag(111) has been studied with density functional theory [29].

Therefore, aiming to create a multifunctional implant coating with anticorrosion, anticancer and antibacterial properties, a systematic density functional theory study of L-glutamine's adsorption sites and intermolecular bonding features on Cu(111) will be performed. The structural and electronic properties of the hybrid system will be analyzed in order to find the potential active sites of L-glutamine and the molecule–Cu or molecule–molecule bonding mechanisms that may lead to a uniform protective coating suitable for orthopedics and orthodontics.

2. Computational Details

We performed standard Kohn–Sham self-consistent density functional theory calculations within the SIESTA code [30,31]. Core electrons were replaced by norm-conserving pseudopotentials in the fully nonlocal Kleinman–Bylander form and the basis set was a general and flexible linear combination of numerical atomic orbitals constructed from the eigenstates of the atomic pseudopotentials [32]. The nonlocal partial core exchange–correlation correction was included for Cu to improve the description of the core valence interactions [33]. An auxiliary real space grid equivalent to a plane-wave cutoff of 100 Ry was used. The Cu surface was simulated using an infinite five layer of (3×8) unit cells corresponding to slabs parallel to the (111) fcc planes, thus resulting in a system having 240 atoms. The system was sampled with 4 $(2 \times 2 \times 1)$ in-plane k -points and a vacuum of 20 Å. L-glutamine was firstly fully relaxed and then softly deposited on the Cu (111) surface. During the geometry optimizations, all atoms were relaxed until the forces between the atoms were less than 0.05 eV/Å, except the latest two layers that were kept fixed, thus mimicking the bulk positions. Using the energetically favored configuration, a second molecule was deposited on Cu(111) parallel or anti-parallel to the first one in order to study the molecule–molecule interactions.

In order to appraise quantitatively the interaction between the molecule and the metallic surface, the binding energy was calculated between L-glutamine and Cu (111) surface using the following equation:

$$E_{\text{binding}} = \frac{E_{\text{total}} - E_{\text{surface}} - nE_{\text{glut}}}{n} \quad (1)$$

where E_{total} is the total energy of the Cu surface together with the adsorbed inhibitor molecule, $E_{surface}$ is the total energy of the Cu surface, E_{glut} is the total energy of the L-glutamine molecule and n is the number of molecules (in our case, $n = 1$ or 2).

DFT Molecular Dynamics (DFT-MD) simulations were also performed using the Verlet algorithm and a time step of 1 femtosecond for 4000 time steps (resulting in a simulation period of 4 picoseconds (psec)) at room temperature to check the vertical and parallel orientation stability of the organic coating.

3. Results and Discussion

3.1. Structural Properties

The structure of the free-standing amino acid L-glutamine was initially optimized starting with a fully aligned C chain configuration. The relaxed configuration reveals the curled carbon chain, as shown in Figure 1a, in excellent agreement with the Cambridge Crystallographic Database (CCDC). In particular, the characteristic distances C_1-O_2 , C_1-N_2 and C_4-C_5 were found 1.296 Å, 1.322 Å and 1.508 Å, respectively, comparable to 1.24 Å, 1.34 Å and 1.54 Å of CCDC database, while the H atoms formed their favored angles ($H-C-H = 105^\circ$) with the C and N atoms.

In order to study the adsorption mechanism, L-glutamine was softly deposited on the Cu (111) surface in six different configurations (I–VI) as shown in Figure 1b–h. Initially, the molecule was aligned horizontally to the surface's [110] direction (configuration I) with its N and O almost over Cu surface atoms (named herein OnTop) as shown in Figure 1b,c. This C atoms' orientation preference along the [110] direction is in line with the lysine amino acid stripes along a [110] direction of Cu(001) [24] and the graphene's zig-zag edge alignment on Cu surfaces [34]. As expected, this configuration was found to be energetically favored showing a binding energy (E_b) of -6.89 eV, Figure 1c. In order to investigate the alternative configurations, the molecule was relaxed along the [110] surface direction having either the C chain shifted from the OnTop sites (configuration II, $E_b = -6.57$ eV) or the N_1 amino group far from the surface and the O_1 and O_2 atoms bonded to the Cu neighboring atoms (configuration III, $E_b = -5.58$ eV), Figure 1d,e, while the alignment along the [211] direction was also considered (configuration IV, $E_b = -3.85$ eV), Figure 1f. Finally, L-glutamine was vertically adsorbed on the surface having the O_3-H_{10} (configuration V, $E_b = -4.49$ eV) or the N_2 amino acid group (configuration VI, $E_b = -4.61$ eV) above the Cu surface atoms as shown in Figure 1g or 1h, respectively. The vertical alignments are the least favored configurations revealing the preference of L-glutamine to adsorb horizontally on the surface. Scanning tunneling microscopy (STM) images revealed that in the solid phase, amino acids lie down on Cu surfaces with the two oxygen atoms and the nitrogen bonded [24]. In addition, electrochemical methods with quantum chemical and molecular dynamics simulations of green corrosion inhibitors for Cu in HCl solution indicate that the orientation of cysteine and alanine amino acids on Cu(111) was almost parallel to the surface and correlated the high inhibition efficiency of cysteine with the Thiol group [23].

The L-glutamine's intramolecular bond lengths and the molecule–surface distance were also evaluated for the energetically favored configuration before and after the energy minimization. The initial free-standing molecule's C_1-O_2 and C_5-O_1 bond lengths are 1.296 Å and 1.246 Å, respectively, while after the molecule's adsorption on the surface, they are shortened to 1.251 Å and 1.229 Å in a good agreement with the basic C–O double bond, 1.23 Å. On the other hand, the C_5-O_3 bond lengthens from 1.32 Å to 1.335 Å compared to the basic C–O single bond, 1.43 Å. Furthermore, the C–N bond length increases by approximately 0.02 Å. In particular, the C_1-N_2 distance increases from 1.322 Å to 1.347 Å while the C_4-N_1 from 1.453 Å to 1.467 Å in good agreement with the general C–N bond 1.479 Å. In addition, although the zig-zag alignment of the carbon chain does not change after the system's energy minimization, the C_2-C_3 and C_3-C_4 bonds or the C_1-C_2 and C_4-C_5 bonds are lengthened by 0.004 Å and 0.02 Å, respectively. Furthermore, in order to describe the L-glutamine/Cu(111) interface structural properties, selective oxygen and nitrogen atoms are chosen and their distance to the first neighboring Cu atoms was measured in the

energetically favored configuration I, Figure 1b,c. The N₁ atom shows the shortest N₁-Cu bond (1.932 Å), while the N₂-Cu distance is 2.609 Å. These results follow the same trend with the N-Fe interatomic distances of other nitrogen-containing amino acids on Fe(110), which were found to be 2.985 Å and 3.112 Å [20]. In addition, the L-glutamine/Cu(111) oxygen distances of O₁-Cu, O₂-Cu and O₃-Cu are 2.165 Å, 2.131 Å and 2.75 Å, respectively, while the O-Fe interatomic lengths of methionine amino acid on Fe(110) range between 2.23 Å and 2.03 Å [21].

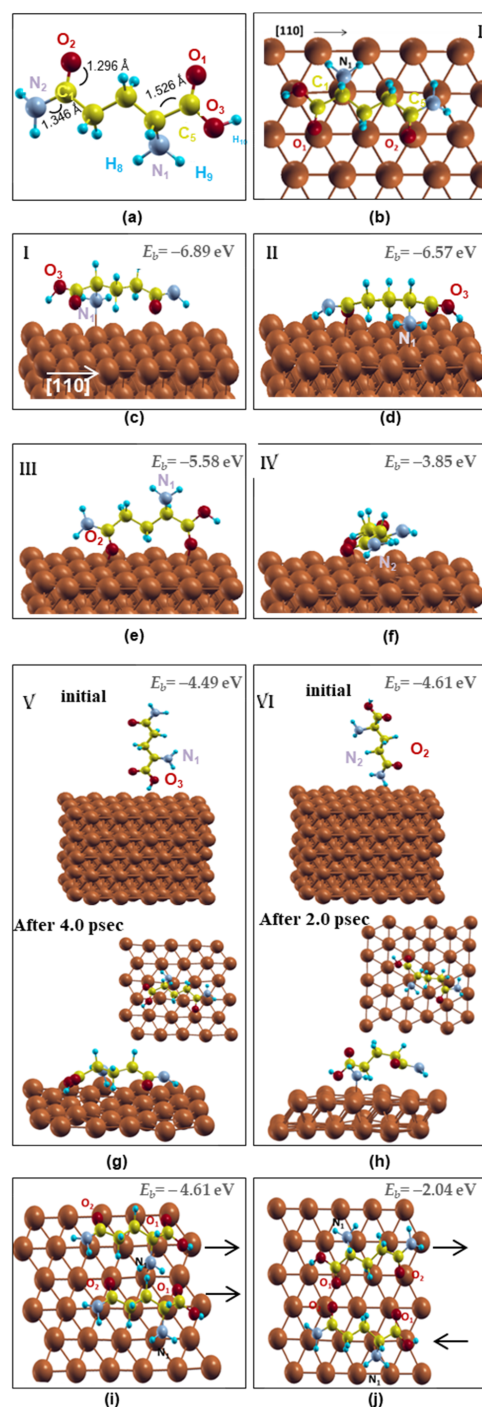


Figure 1. Schematic representation of the several adsorption sites of L-glutamine molecule(s) on Cu (111) surface. (a) Optimized structure of L-glutamine; (b) OnTop view and (c) side view of L-glutamine in OnTop site along [110]; (d) molecule slightly shifted from OnTop site; (e) N₁ amino

group far from the surface; (f) L-glutamine along [211]; (g,h) vertical alignments toward the surface (upper insets) and snapshots of DFT-MD simulations (lowest insets); (i) and (j) two molecules aligned parallel and antiparallel along [110], respectively. The black arrows show the orientation of the molecules. Grey, yellow, red, blue and brown balls stand for the N, C, O, H and Cu atoms, respectively.

In summary, the favored L-glutamine adsorption site on Cu(111) is the OnTop that aligns the carbon chain along the [110] direction of Cu(111), resulting in a highly bonded interaction with the amino group of the molecule's backbone through Cu-N₁ along with short on top oxygen sites for the O₁ and O₂ atoms, Figure 1b,c. The N₁-Cu, O₁-Cu and O₂-Cu interatomic distances are shorter than the N-Fe and O-Fe lengths of similar amino acids on Fe(110) [20,21], revealing the importance of the small lattice mismatch between the C chain and the metallic surface, as presented in Figure 1b, in line with the graphene adsorption on Cu surfaces [34].

DFT Molecular Dynamics (DFT-MD) simulations were also performed in order to determine whether the horizontal alignment persists at high temperatures. Several initial configurations were studied revealing remarkable results. In line with the energy minimization results, the MD simulations for the OnTop and all horizontal configurations retain the L-glutamine horizontally aligned on the Cu(111) surface for a duration of 2 psec at room temperature. On the contrary, both L-glutamine's vertical positions on Cu(111) surface required less than 2 psec at room temperature to rotate horizontally on the surface as shown in the lowest insets of Figure 1g,h. In particular, in the first vertical configuration (Figure 1g), the L-glutamine's O₃ atom relaxes closer to the surface, while in the second one, the N₁ and O₃ atoms lie towards the Cu(111) with the alkyl chain relaxed outwards (Figure 1h). It should be noted that in both configurations, the L-glutamine relaxes along the [110] directions of the Cu(111) surface at 300 K following the energetically favored OnTop arrangement found at zero temperature. Indeed, L-glutamine's N and/or O are located at the OnTop sites over Cu surface atoms, while the C chain relaxes along the [110] direction, insets of Figure 1g,h. These results support the horizontal coating of L-glutamine on the Cu (111) surface, the importance of the C chain alignment along the [110] direction and the relaxation of O or N atoms at OnTop sites.

Since the L-glutamine can adsorb on Cu(111) surface through its functional groups N and O, we continued our DFT calculations similarly depositing two molecules that interact and almost cover the computational surface layer creating in this way an organic coating. Choosing the energetically favored configuration of L-glutamine having the N and O atoms "on top" of Cu atoms, we deposited the two molecules aligned parallel or antiparallel as shown in Figure 1i,j, respectively. The binding energy of the parallel configuration, Figure 1i, is lower than the antiparallel one, Figure 1j, rendering, therefore, the first alignment energetically favored for organic coating on Cu(111).

3.2. Electronic Properties

The electronic properties of the energetically favored configuration of L-glutamine on the Cu(111) surface were investigated in order to reveal the bonding hybridizations. Figure 2a shows the system's total electronic density of states (EDOS) with solid lines and the projection of the wavefunction (WF) onto the Cu's *d* orbitals with dashed lines. The contribution of the system's *p* orbitals and *s* orbitals at each energy state is shown in Figure 2b,c, respectively. The Fermi energy is set to zero and the energy values are shifted with respect to the Fermi level. The Cu's electron states are shown to be basically responsible for the occupation around the Fermi level, while L-glutamine's electrons are mainly responsible for the lower energy states. More specifically, there is a main peak at the energy range from -1 eV to -9 eV due to Cu's *d* electrons, which is in agreement with the bulk Cu's behavior. The energy range from -2 eV to -12 eV is mainly due to the L-glutamine's N, O and C *p* electrons' occupation, while the density of states around -13 eV, -15 eV, -17 eV and -20 eV are due to the corresponding *s* electrons. For all energies, the H *s* electrons have the smallest occupation. Both surface and amino acid atoms

contribute in the energy range from -3 eV to -6 eV, suggesting the existence of electron hybridizations. The higher contribution of N, C and O p orbitals indicates the ability of these functional groups to form bonds with the substrate that theoretically was proved for the iron surfaces [25]. For this reason, bonded states are expected to be found in lower energies and especially in the energy range, where both surface's and L-glutamine's atoms participate. Similar behavior was found for the EDOS of the two L-glutamines on Cu(111). In particular, Copper electrons are mostly responsible for the Fermi level states, while in lower energy states the L-glutamines' atoms mainly contribute, similar to the single case. Moreover, all atoms contribute to the energy states from -3.5 eV to -9 eV, while the EDOS peaks of the two L-glutamine molecules on Cu are lower and wider compared to the one L-glutamine case indicating intermolecular interactions.

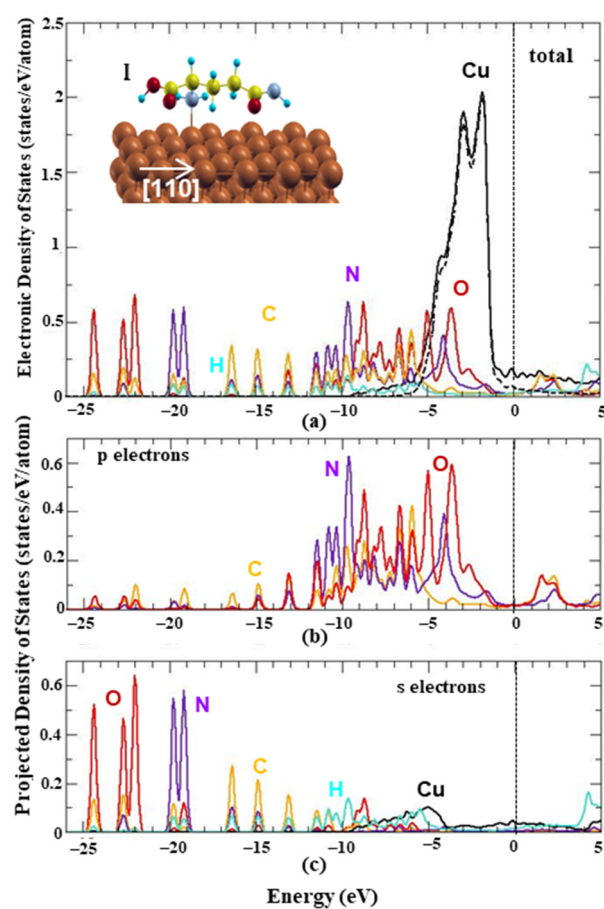


Figure 2. Total and projected electronic density of states of L-glutamine on Cu(111). (a) Total electronic density of states for each element of the energetically favored configuration (OnTop site). The black dashed line stands for Cu's d electrons. (b) Projected wavefunctions on the system's p electrons and (c) s electrons. For each panel, black, orange, red, purple and light blue solid lines stand for Cu, C, O, N and H, respectively. Vertical dashed black lines show the fermi level that is set to zero.

Aiming to identify the molecule's active sites and the bonded hybridizations, the L-glutamine's electronic structure was further studied. Certain electronic structure parameters have been correlated with the effectiveness of adsorption-type inhibitors, including the energies of the highest occupied molecular orbital (HOMO) and the lowest unoccupied molecular orbital (LUMO), as well as the corresponding HOMO-LUMO energy gap (E_{gap}) [21]. It is well known that comparing several inhibitors, the highest E_{HOMO} value indicates a tendency of one molecule to donate electrons to appropriate acceptor molecules. The LUMO energy characterizes the propensity of the molecule towards attack by nucleophiles; therefore, the lowest value of E_{LUMO} indicates the electron-accepting

ability of an inhibitor molecule compared to other molecules. Therefore, the binding ability of an inhibitor to a metal surface increases while increasing E_{HOMO} and decreasing E_{LUMO} [17,20,21]. In Table 1, the L-glutamine's E_{HOMO} (−5.74 eV) and E_{LUMO} (−1.72 eV) energies are in good agreement with other quantum chemical methods [14,17]. Although in this work only L-glutamine has been studied on Cu(111), the results of the free-standing L-glutamine HOMO, LUMO and total energy are given in Table 1 for comparison reasons. In addition, since it is difficult to compare the single-molecule HOMO (LUMO) energy values with the corresponding adsorbed ones (due to the Cu electron states introduction), the L-glutamine/Cu(111)'s WFs will be investigated in order to reveal the system eigenvalues, where the molecule dominates as well as the available bonding energy states.

Table 1. L-glutamine's HOMO and LUMO unshifted energies ($E_{\text{F}} = -3.17$ eV) and E_{gap} along with available theoretical data. In parenthesis, the HOMO- and LUMO-shifted energies with respect to the fermi level ($E_{\text{F}} = 0$ eV) are presented.

L-Glutamine	HOMO (eV)	LUMO (eV)	Egap (eV)
Present work	−5.74 (−1.89)	−1.72 (2.13)	4.02
DFT [16]	−5.69	−2.11	3.58
Quant. Chem. [26]	−5.54	−1.66	3.88
DFT [19]	−6.19	0.92	7.11

Starting with the free-standing L-glutamine, the HOMO and LUMO states are presented in Figure 3a. The HOMO is found to be located mainly around the backbone's N_1 atom showing N-2p character, while the backbone's O_1 , O_3 and C_5 p electrons are mostly responsible for the LUMO WF indicating that N_1 can provide electrons while O_1 , O_3 and C_5 can accept electrons. These observations are in good agreement with other theoretical studies on L-glutamine's electronic properties on steel [17].

Upon L-glutamine's adsorption on Cu(111), the free molecule's HOMO electronic features are altered (Figure 3b). As shown in the EDOS, Figure 2, close to the fermi level ($E_{\text{F}} = 0$ eV), the Cu-4s and Cu-3d electrons make significant contributions, while the N-2p, O-2p, C-2p and H-1s also participate with lower electron occupation. This is reflected in Figure 3b (system's highest occupied state, HOS), where the Cu-4s electrons mainly occupy the distance to the molecule atoms, while localization of the Cu-3d orbital in the molecule's neighborhood is observed. The L-glutamine's states are depleted. The O-2p and N-2p electrons are weakly occupied showing dangling bonds (red lobes), which are not hybridized with the Cu-3d substrate's blue lobes, revealing weak interaction at HOS (−0.04 eV). To reveal the existence of molecule–metal bonding hybridizations, the system's WFs were investigated at more localized states. In Figure 3c–e, the WFs at energies −4.99 eV, −5.30 eV and −5.79 eV ($E_{\text{F}} = 0$ eV) were selected, where the L-glutamine forms remarkable directional bonds with the Cu substrate mainly through the backbone's N_1 atom, which interestingly shows the highest electron occupation in the single-molecule HOMO state, Figure 3a, denoting its property as an active center. In particular, the N_1-2p orbital is hybridized with the Cu-3d electrons forming a directional orbital (red or blue charge areas) shown by the yellow dashed line in Figure 3c–e. This is in excellent agreement with the behavior of L-glutamine and other N-containing organic compounds adsorbed on metallic surfaces [17,20,25]. Furthermore, the O_1-2p orbital is also bonded to the Cu-3d at −5.30 eV along with the N_1-2p , as presented in Figure 3d through a long blue charge area (red dashed line) in the interface. In Figure 3e, the lowest presented energy (−5.79 eV) reveals C-2p and Cu-3d bonding hybridizations along with the N_1-2p ones, showing strong interaction between L-glutamine and Cu(111) via two different functional groups. It should be noted that the Cu-3d electrons mainly contribute to these bonding states against the Cu-4s electrons. These low-energy hybridizations reveal the strong interaction of L-glutamine on the Cu surface, showing that this molecule can indeed act as the substrate's corrosion inhibitor. These results are in line with the characteristic amino acids' adsorption chemical bonding on metallic surfaces [17].

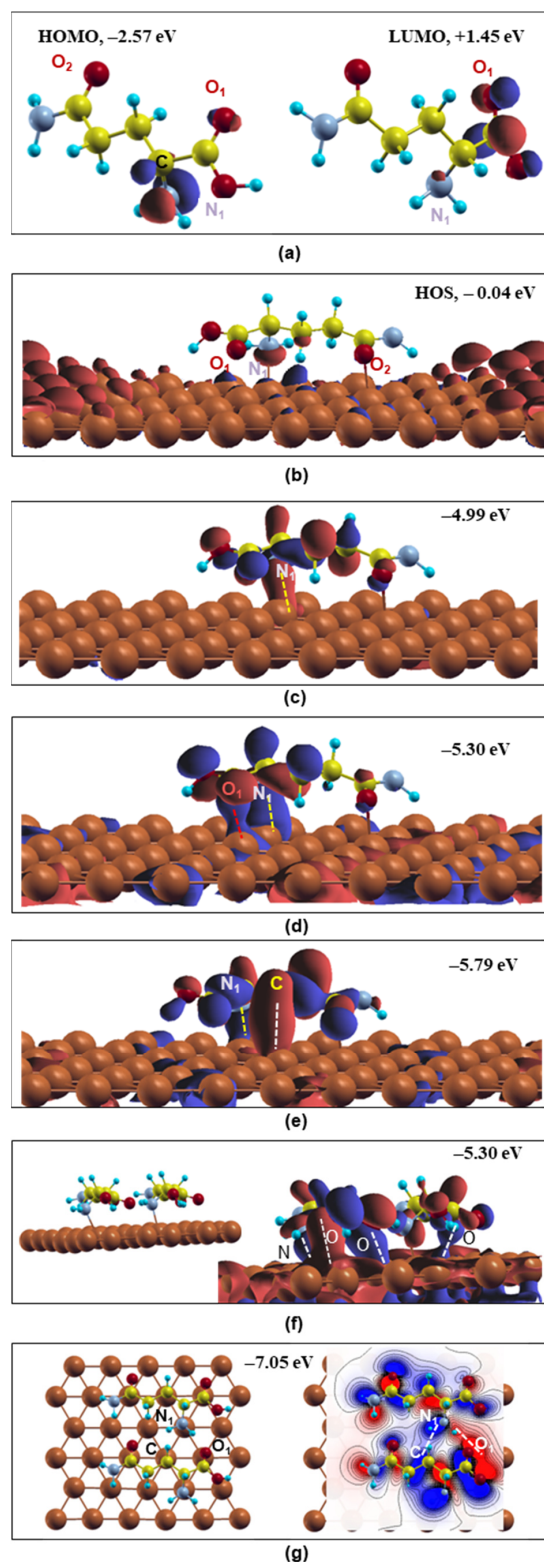


Figure 3. Optimized free L-glutamine molecule's and molecule(s)/Cu (111) system's wavefunctions. (a) Free molecule's HOMO and LUMO; (b–e) optimized wavefunctions of L-glutamine on Cu(111); (f) side view of the two L-glutamine molecules/Cu(111) system (left) and the system's optimized wavefunction at -5.30 eV(right); (g) OnTop view of the two adsorbed molecules (left) and 2d representation of the electron density contribution between the molecules at -7.05 eV (right). Red and blue colors indicate particular isosurfaces at positive and negative values, respectively. Dashed lines show the bonding behavior of the atoms. Grey, yellow, red, blue and brown balls stand for the N, C, O, H and Cu atoms, respectively.

The two L-glutamine WFs show similar features to the single molecule. At the fermi level, the WFs are dominant by the Cu's surface electrons without metal–molecule hybridizations. On the contrary, below -3.5 eV, both L-glutamine molecules may participate in the WFs using their functional groups forming directional bonds with the Cu substrate. In particular in Figure 3f, one L-glutamine forms bonds with the N-p and O-p electrons of its backbone and the other molecules make hybridizations with the O-p of its sidechain with the Cu's *d* orbitals (denoted by dashed white lines) similar to the single molecule, Figure 3d. In addition, molecules/metal hybridizations are found in several energy states from -3 eV to -6 eV, where the charge distribution is not always similar on both molecules. Furthermore, the C atoms may participate in bonding with the surface atoms, a feature that was not so clear in the single-molecule case, similar to other organic compounds that form coordinate bonds through their carbon atoms with the Fe surface's atoms [20]. In addition to this, it is mentioned in the literature that the $-C=O$ carbonyl group is operative in a back-donation process for the cysteine deposited on the Cu(111) surface [17]. Finally, in Figure 3g, the WF at -7.05 eV offers the intermolecular directional bonds between the N_1-p electrons of one molecule and the C and O_1 electrons of the second L-glutamine as denoted by a dashed line. Similar intermolecular hybridizations have been also observed in higher energy states starting from -3.30 eV revealing the strong molecule–molecule covalent-like interactions. These molecule/metal and the intermolecular directional covalent-like bonds will result in a stable and continuous organic coating on the Cu(111) surface. It should be noted that potentiodynamic polarization and electrochemical impedance spectroscopy (EIS) revealed glutamine on Cu in HCl having the highest inhibition efficiency against asparagine, glutamic acid and aspartic acid, while this Cu corrosion protection increases with molecule concentration [22]. These experimental data are in line with the results of this work concerning the highest number of covalent-like bonding of the two L-glutamines on Cu, Figure 3.

The EDOS and WFs results are supported by the Mulliken analysis. Indeed, charge transfer was found from the molecule's bonded to the surface N ($0.2 e^-$), C ($0.4 e^-$) atoms and Cu (0.07 – $0.08 e^-$) neighboring atoms towards the O ($0.3 e^-$) atoms. This is in line with the single L-glutamine's HOMO that was mostly around the backbone's N, while the LUMO was found around O indicating their ability to donate and accept electrons, respectively. Therefore, the Mulliken analysis supports the propensity of the molecule to accept electrons in order to form feedback bonds when deposited on the surface and acts as its corrosion inhibitor. Similar behavior was obtained for the two molecules' case. Particularly, the charge was transferred from both molecules' N and C as well as neighboring Cu atoms towards the two molecules' oxygen atoms.

4. Conclusions

L-glutamine's energetically favored configuration is the one with the C zig-zag chain aligned horizontally to the [110] surface direction, having the N atoms and the oxo-group O atoms laying almost on top of Cu(111) surface atoms. Considering this single molecule's favored deposition site, an extra L-glutamine molecule prefers the parallel alignment, while considering the in-plane periodic boundary conditions, an almost full two-dimensional organic coating can be achieved.

The electronic properties of the hybrid system reveal a HOMO state with localized Cu-3d electrons in the neighborhood of the L-glutamine. The electronic total and projected density of states retain the general features of the pure components showing an enhanced broad Cu peak from -1 eV to -9 eV, while the major molecule–metal hybridizations were found around the energy range from -3 eV up to -6 eV. These results are depicted in the corresponding wavefunctions, where L-glutamine's N, O and C atoms form remarkably directional bonds with the Cu surface atoms below -3 eV, indicating their enhanced interaction. Interestingly, L-glutamine is mainly bonded through the backbone's N_1 atom, which shows the highest electron occupation in the single-molecule HOMO state, denoting its property as an active center. Similar behavior is found for the two L-glutamine EDOS

and WFs, while the intermolecular bonds that were depicted below -3.30 eV reveal a strong and stable organic coating. The electronic properties are supported by the Mulliken analysis, where charge transfer from the molecule's N, C and Cu neighboring atoms towards the O atoms was found in line with the single-molecule HOMO-LUMO features.

In conclusion, L-glutamine organic coating can successfully form on Cu(111) due to the molecule's preference to align horizontally, forming a well-localized, directional covalent-like intermolecular and metal–molecule bonds. These results could be used for the creation of multifunctional organic–metallic coatings with corrosion resistance, antibacterial and anticancer properties for many technological applications.

Author Contributions: M.B.: data curation, writing—original draft preparation. C.L.: supervision, writing—review and editing. All authors have read and agreed to the published version of the manuscript.

Funding: Christina Lekka is grateful for the financial support from the European Commission within the H2020-MSCA grant agreement No. 861046 (BIOREMIA-ITN).

Data Availability Statement: Data is contained within the article

Conflicts of Interest: The authors declare no conflict of interest.

References

1. Li, S.; Meng, L.; Zhu, Y.; Zhang, W.; Sun, Y.; Bai, G.; Li, X. Copper ion-loaded surface charge-convertible coatings on implant: Antibacterial and tunable cell adhesion properties. *Chem. Eng. J.* **2023**, *478*, 147439. [[CrossRef](#)]
2. Wu, Y.; Zhou, H.; Zeng, Y.; Xie, H.; Ma, D.; Wang, Z.; Liang, H. Recent Advances in Copper-Doped Titanium Implants. *Materials* **2022**, *15*, 2342. [[CrossRef](#)]
3. Liu, S.; Zhang, Z.; Zhang, J.; Qin, G.; Zhang, E. Construction of a TiO₂/Cu₂O multifunctional coating on Ti-Cu alloy and its influence on the cell compatibility and antibacterial properties *Surf. Coat. Technol.* **2021**, *421*, 127438. [[CrossRef](#)]
4. Zhang, L.; Guo, J.; Huang, X.; Zhang, Y.; Han, Y. The dual function of Cu-doped TiO₂ coatings on titanium for application in percutaneous implants. *J. Mater. Chem. B* **2016**, *4*, 3788. [[CrossRef](#)] [[PubMed](#)]
5. Akman, A.; Alberta, L.A.; Giraldo-Osorno, P.L.; Turner, A.B.; Hantusch, M.; Palmquist, A.; Trobos, M.; Calin, M.; Gebert, A. Effect of minor gallium addition on corrosion, passivity, and antibacterial behaviour of novel b-type Ti-Nb alloys. *J. Mater. Res. Technol.* **2023**, *25*, 4110. [[CrossRef](#)]
6. Alberta, L.A.; Fortouna, Y.; Vishnu, J.; Pilz, S.; Gebert, A.; Lekka, C.E.; Nielsch, K.; Calin, M. Effects of Ga on the structural, mechanical and electronic properties of β -Ti45Nb alloy by experiments and ab initio calculations. *J. Mech. Behav. Biomed. Mater.* **2023**, *140*, 105728. [[CrossRef](#)] [[PubMed](#)]
7. Alberta, L.A.; Vishnu, J.; Hariharan, A.; Pilz, S.; Gebert, A.; Calin, M. Novel low modulus beta-type TiNb alloys by gallium and copper minor additions for antibacterial implant applications. *J. Mater. Res. Technol.* **2022**, *20*, 3306. [[CrossRef](#)]
8. Fateh, A.; Aliofkhaezai, M.; Rezvani, A.R. Review of corrosive environments for copper and its corrosion inhibitors *Arab. J. Chem.* **2020**, *13*, 481.
9. Demadis, K.D.; Mavredaki, E.; Stathouloupoulou, A.; Neofotistou, E.; Mantzaridis, C. Industrial water systems: Problems, challenges and solutions for the process industries. *Desalination* **2007**, *213*, 38. [[CrossRef](#)]
10. Dariva, C.G.; Galio, A.F. Corrosion Inhibitors—Principles, Mechanisms and Applications. In *Developments in Corrosion Protection*; Aliofkhaezai, M., Ed.; IntechOpen: London, UK, 2014; pp. 365–379. [[CrossRef](#)]
11. Popoola, A.; Olorunniwo, O.E.; Ige, O.O. Corrosion Resistance through the Application of Anti-Corrosion. In *Developments in Corrosion Protection*; Aliofkhaezai, M., Ed.; IntechOpen: London, UK, 2014; pp. 241–270. [[CrossRef](#)]
12. Fu, J.J.; Li, S.N.; Cao, L.H.; Wang, Y.; Yan, L.H.; Lu, L.D. L-Tryptophan as green corrosion inhibitor for low carbon steel in hydrochloric acid solution. *J. Mater. Sci.* **2010**, *45*, 979. [[CrossRef](#)]
13. Obot, I.B.; Obi-Egbedi, N.O. Adsorption properties and inhibition of mild steel corrosion in sulphuric acid solution by ketoconazole: Experimental and theoretical investigation. *Corros. Sci.* **2010**, *52*, 198. [[CrossRef](#)]
14. Singh, A.; Ebenso, E.E. Use of Glutamine as a New and Effective Corrosion Inhibitor for Mild Steel in 1 M HCL Solution. *Int. J. Electrochem. Sci.* **2013**, *8*, 12874. [[CrossRef](#)]
15. Khaled, K.F. Corrosion control of copper in nitric acid solutions using some amino acids—A combined experimental and theoretical study. *Corros. Sci.* **2010**, *52*, 3225. [[CrossRef](#)]
16. Belghiti, M.E.; Echihi, S.; Dafali, A.; Karzazi, Y.; Bakasse, M.; Elalaoui-Elabdallaoui, H.; Olasunkanmi, L.O.; Ebenso, E.E.; Tabyaoui, M. Computational simulation and statistical analysis on the relationship between corrosion inhibition efficiency and molecular structure of some hydrazine derivatives in phosphoric acid on mild steel surface. *Appl. Surf. Sci.* **2019**, *491*, 707. [[CrossRef](#)]
17. Oguike, R.S.; Oni, O. Computational Simulation and Inhibitive Properties of Amino Acids for Mild Steel Corrosion: Adsorption in Gas Phase onto Fe (110). *Int. J. Res. Chem. Environ.* **2014**, *4*, 177–186.

18. Kabanda, M.M.; Obot, I.B.; Ebenso, E.E. Computational Study of Some Amino Acid Derivatives as Potential Corrosion Inhibitors for Different Metal Surfaces and in Different Media. *Int. J. Electrochem. Sci.* **2013**, *8*, 10839. [[CrossRef](#)]
19. Zarrouk, A.; Zarrok, H.; Salghi, R.; Hammouti, B.; Al-Deyab, S.S.; Touzani, R.; Bouachrine, M.; Warrad, I.; Hadda, T.B. A Theoretical Investigation on the Corrosion Inhibition of Copper by Quinoxaline Derivatives in Nitric Acid Solution. *Int. J. Electrochem. Sci.* **2012**, *7*, 6353. [[CrossRef](#)]
20. Xia, S.; Qiu, M.; Yu, L.; Liu, F.; Zhao, H. Molecular dynamics and density functional theory study on relationship between structure of imidazoline derivatives and inhibition performance. *Corros. Sci.* **2008**, *50*, 2021. [[CrossRef](#)]
21. Oguzie, E.E.; Li, Y.; Wang, S.G.; Wang, F. Understanding corrosion inhibition mechanisms—Experimental and theoretical approach. *RSC Adv.* **2011**, *1*, 866. [[CrossRef](#)]
22. Zhang, D.Q.; Cai, Q.R.; Hea, X.M.; Gao, L.X.; Zhou, G.D. Inhibition effect of some amino acids on copper corrosion in HCl solution. *Mater. Chem. Phys.* **2008**, *112*, 353. [[CrossRef](#)]
23. Milošev, I.; Pavlinac, A.; Hodošček, M.; Lesar, A. Amino acids as corrosion inhibitors for copper in acidic medium: Experimental and theoretical study. *J. Serb. Chem. Soc.* **2013**, *78*, 2069. [[CrossRef](#)]
24. Zhao, X.Y.; Wang, H.; Yan, H.; Gai, Z.; Zhao, R.G.; Yang, W.S. Adsorption behavior of amino acids on Copper surfaces. *Chin. Phys. Soc.* **2001**, *10*, 1009.
25. Zhang, Z.; Chen, S.; Feng, Y.; Ding, Y.; Zhou, J.; Jia, H. Electrochemical and molecular simulation studies on the corrosion inhibition of L-glutamine monolayers on an iron surface. *J. Serb. Chem. Soc.* **2009**, *74*, 407. [[CrossRef](#)]
26. Eddy, N.O. Experimental and theoretical studies on some amino acids and their potential activity as inhibitors for the corrosion of mild steel, Part 2. *J. Adv. Res.* **2011**, *2*, 35. [[CrossRef](#)]
27. Eddy, N.O. Part 3. Theoretical study on some amino acids and their potential activity as corrosion inhibitors for mild steel in HCl. *Mol. Simul.* **2010**, *36*, 354. [[CrossRef](#)]
28. Jin, J.; Byun, J.K.; Choi, Y.K.; Park, K.G. Targeting glutamine metabolism as a therapeutic strategy for cancer. *Nat. Exp. Mol. Medicine.* **2023**, *55*, 706. [[CrossRef](#)]
29. Maurer, R.J.; Ruiz, V.G.; Camarillo-Cisneros, J.; Liu, W.; Ferri, N.; Reuter, K.; Tkatchenko, A. Adsorption structures and energetics of molecules on metal surfaces: Bridging experiment and theory. *Prog. Surf. Sci.* **2016**, *91*, 2–72. [[CrossRef](#)]
30. Artacho, E.; Sanchez-Portal, D.; Ordejon, P.; Garcia, A.; Soler, J.M. Linear-Scaling ab-initio Calculations for Large and Complex Systems. *Phys. Status Solidi B* **1999**, *215*, 809. [[CrossRef](#)]
31. Perdew, J.P.; Zunger, A. Self-Interaction Correction to Density-Functional Approximations for Many-Electron Systems. *Phys. Rev. B* **1981**, *23*, 5048. [[CrossRef](#)]
32. Troullier, N.; Martin, J.L. Efficient pseudopotentials for plane-wave calculations, *Phys. Rev. B* **1991**, *43*, 1993. [[CrossRef](#)]
33. Junquera, J.; Paz, O.; Sanchez-Portal, D.; Artacho, E. Numerical atomic orbitals for linear-scaling calculations. *Phys. Rev. B* **2001**, *64*, 235111. [[CrossRef](#)]
34. Murdock, A.T.; Koos, A.; Britton, T.B.; Houben, L.; Batten, T.; Zhang, T.; Wilkinson, A.J.; Dunin-Borkowski, R.E.; Lekka, C.E.; Grobert, N. Controlling the Orientation, Edge Geometry, and Thickness of Chemical Vapor Deposition Graphene. *ACS Nano* **2013**, *7*, 1351. [[CrossRef](#)] [[PubMed](#)]

Disclaimer/Publisher’s Note: The statements, opinions and data contained in all publications are solely those of the individual author(s) and contributor(s) and not of MDPI and/or the editor(s). MDPI and/or the editor(s) disclaim responsibility for any injury to people or property resulting from any ideas, methods, instructions or products referred to in the content.